frontiers | Frontiers in Cardiovascular Medicine

TYPE Original Research
PUBLISHED 29 November 2023
DOI 10.3389/fcvm.2023.1233712

OPEN ACCESS

EDITED BY
Claire S. Whyte,
University of Aberdeen, United Kingdom

REVIEWED BY
Devesh Rai,
Rochester General Hospital, United States
Adria Arboix,
Sacred Heart University Hospital, Spain

*CORRESPONDENCE
Beatriz Eguzkitza
✉ beatriz.eguzkitza@bsc.es

RECEIVED 02 June 2023
ACCEPTED 15 September 2023
PUBLISHED 29 November 2023

CITATION
Eguzkitza B, Oks D, Navia JA, Houzeaux G, Butakoff C, Fisa M, Campoy Millán A and Vázquez M (2023) Performance assessment of an electrostatic filter-diverter stent cerebrovascular protection device. Is it possible not to use anticoagulants in atrial fibrilation elderly patients?
Front. Cardiovasc. Med. 10:1233712.
doi: 10.3389/fcvm.2023.1233712

Performance assessment of an electrostatic filter-diverter stent cerebrovascular protection device. Is it possible not to use anticoagulants in atrial fibrilation elderly patients?

Beatriz Eguzkitza[1]*, David Oks[1,4], José A. Navia[2], Guillaume Houzeaux[1,3], Constantine Butakoff[3], María Fisa[3,4], Ariadna Campoy Millán[3,5,6] and Mariano Vázquez[1,3]

[1]Barcelona Supercomputing Center, Computer Applications in Science and Engineering, Barcelona, Spain, [2]Cardiac Surgery Service Department, University Hospital (Austral University), Buenos Aires, Argentina, [3]ELEM Biotech SL, Barcelona, Spain, [4]Bioengineering Department, Universitat Pompeu Fabra, Barcelona, Spain, [5]Bioengineering Department, Universitat de Barcelona, Barcelona, Spain, [6]Bioengineering Department, Universitat Politècnica de Catalunya, Barcelona, Spain

Stroke is the second leading cause of death worldwide. Nearly two-thirds of strokes are produced by cardioembolisms, and half of cardioembolic strokes are triggered by Atrial Fibrillation (AF), the most common type of arrhythmia. A more recent cause of cardioembolisms is Transcatheter Aortic Valve Replacements (TAVRs), which may onset post-procedural adverse events such as stroke and Silent Brain Infarcts (SBIs), for which no definitive treatment exists, and which will only get worse as TAVRs are implanted in younger and lower risk patients. It is well known that some specific characteristics of elderly patients may lower the safety and efficacy of anticoagulation therapy, making it a real urgency to find alternative therapies. We propose a device consisting of a strut structure placed at the base of the treated artery to model the potential risk of cerebral embolisms caused by dislodged debris of varying sizes. This work analyzes a design based on a patented medical device, intended to block cardioembolisms from entering the cerebrovascular system, with a particular focus on AF, and potentially TAVR patients. The study has been carried out in two stages. Both of them based on computational fluid dynamics (CFD) coupled with Lagrangian particle tracking method. The first stage of the work evaluates a variety of strut thicknesses and inter-strut spacings, contrasting with the device-free baseline geometry. The analysis is carried out by imposing flowrate waveforms characteristic of both healthy and AF patients. Boundary conditions are calibrated to reproduce physiological flowrates and pressures in a patient's aortic arch. In the second stage, the optimal geometric design from the first stage was employed, with the addition of lateral struts to prevent the filtration of particles and electronegatively charged strut surfaces, studying the effect of electrical forces on the clots if they are considered charged. Flowrate boundary conditions were used to emulate both healthy and AF conditions. Results from numerical simulations coming form the first stage indicate that the device blocks particles of sizes larger than the inter-strut spacing. It was found that lateral strut space had the highest impact on efficacy. Based on the results of the second stage, deploying the electronegatively charged device in all three aortic arch arteries, the number of particles entering these arteries was reduced on average by 62.6% and 51.2%, for the healthy and diseased models

respectively, matching or surpassing current oral anticoagulant efficacy. In conclusion, the device demonstrated a two-fold mechanism for filtering emboli: while the smallest particles are deflected by electrostatic repulsion, avoiding microembolisms, which could lead to cognitive impairment, the largest ones are mechanically filtered since they cannot fit in between the struts, effectively blocking the full range of particle sizes analyzed in this study. The device presented in this manuscript offers an anticoagulant-free method to prevent stroke and SBIs, imperative given the growing population of AF and elderly patients.

KEYWORDS

computational fluid dynamics modeling (CFD), atrial fibrillation, TAVR, silent brain infarcts, stroke, particle flow simulation, cerebroembolic protection devices, aortic arch

1. Introduction

Stroke is the second leading cause of death worldwide (1). Nearly two-thirds of strokes are produced by cardioembolisms (2). Cardioembolic strokes are caused by blood clots that form in the heart, due to disease (e.g., atrial fibrillation) or a cardiac intervention (e.g., transcatheter aortic valve replacements or left atrial appendage occluders), and travel through the bloodstream into the brain. Half of the cardioembolic strokes are caused by Atrial Fibrillation (AF), a heart condition that causes an irregular and often abnormally fast heart rate with a significant reduction in the cardiac output (20%). It is proven that this dysfunction increases the propensity of emboli, which tend to travel through the Brachiocephalic Trunk (BCT), Left Carotid Common Artery (LCCA), and Left Subclavian Artery (LSA compromising the flow of the left vertebral artery), to the brain, obstructing the superior arteries and triggering cerebral strokes (3).

1.1. Why is atrial fibrillation a critical problem?

AF is the most common heart rhythm disorder, responsible for approximately one-third of hospitalizations for cardiac rhythm disturbances in the US. The prevalence and incidence of AF are increasing. It is predicted to affect 6-12 million people in the US by 2050 and 17.9 million in Europe by 2060, significantly impacting wellbeing and healthcare costs. AF is associated with increased morbidity and mortality, due to the risk of ischemic stroke, systemic embolism, heart failure, and cognitive impairment, reducing the quality and quantity of life in these patients (4). This condition is associated with a six-fold increase in stroke. Moreover, patients with previous ischemic stroke are at an even higher risk (5). In the case of cardioembolic strokes (two-thirds of the total), echocardiographic and pathologic studies suggest that when a source can be identified, approximately 90% of such strokes can be attributed to thrombus formation in the left atrial appendage (2). Non-rheumatic AF is the most frequent source of cardioembolic brain infarct (57.1% of cases) followed by valvular heart disease (20.3%) and coronary artery disease (18.2%), that AF can also occur in patients with atherothrombotic stroke as epiphenomenon or as clinical manifestation of atherosclerotic disease (16.5%). In-hospital mortality in patients with atrial fibrillation was significantly higher than in non-atrial fibrillation patients both in cardioembolic (32.6% vs. 14.8%, $P < 0.005$) and atherothrombotic stroke (29.3% vs. 18.8%, $P < 0.04$). Valvular heart disease, and sudden onset (OR 1.8; 95% CI 0.97–3.63) were predictors of cardioembolic stroke, and subacute onset, (Chronic obstructive pulmonary disease), hypertension, hypercholesterolemia, transient ischaemic attack, ischaemic heart disease, diabetes of atherothrombotic stroke (6). Bayés syndrome (Bayés de Luna 1988) is a new clinical entity, characterized by the association of advanced interatrial block (IAB) on surface electrocardiogram with AF and other atrial arrhythmias. This syndrome is associated with an increased risk of stroke, dementia, and mortality. Recent studies have shown that Bayés syndrome is a key independent factor of cardioembolic cerebral ischemia[, although there is still a need for a high level of clinical suspicion in order to diagnose it. Early and proper diagnosis of Bayés syndrome is desirable and necessary since patients will require closer clinical surveillance, and possibly accompanying antiarrhythmic and antithrombotic preventive therapies. The clinical relevance of Bayés syndrome lies in the fact that is a clear arrhythmological syndrome and has a strong association with supraventricular arrhythmias, particularly atypical atrial flutter and atrial fibrillation. Likewise, Bayés syndrome has been recently identified as a novel risk factor for non-lacunar cardioembolic ischemic stroke and vascular dementia (7).

1.2. What are the existing treatments for stroke and what are their drawbacks?

The primary approach to prevent ischaemic stroke risk associated with AF, are anticoagulation therapies, which have a proven efficacy. At least four large clinical trials have clearly demonstrated that anticoagulation with warfarin decreases the risk of stroke by 50–80% (8–11). In relatively recent trials, the newer oral anticoagulants (OACs), such as dabigatran, rivaroxaban, apixaban, and edoxaban, have proven to be similarly effective to warfarin for the prevention of stroke and thromboembolism (12). However, anticoagulants have significant drawbacks. Although anticoagulants reduce 30-day mortality from ischaemic stroke, these agents increase intracranial haemorrhage-related mortality (13). Moreover, patients having a

stroke despite being on therapy with an oral anticoagulant are at high risk of recurrent ischaemic strokes (14). In the ANAFIE registry, patients at high bleeding risk had higher incidences of stroke, major bleeding, intracranial haemorrhage, gastrointestinal bleeding, cardiovascular events, and all-cause death than patients in the reference group, despite a high prevalence of OAC therapy (89.0%) (15). In elderly patients, non-adherence to OAC treatment, associated commorbidities and additional risk factors can significantly increase the incidence and severity of cerebrovascular accidents. In this age group, a delicate balance may exist between multiple conditions, being thrombotic disease, chronic kidney disease, cancer, coronary artery disease, and heart failure, some of the most challenging scenarios encountered in clinical practice (15). In addition, warfarin OACs have multiple contraindications (16):

- prior intracranial haemorrhage or diseases predisposing to intracranial haemorrhage,
- active gastrointestinal bleeding or diseases predisposing to gastrointestinal bleeding (such as active ulcer), or inflammation of the gastrointestinal tract,
- anaemia, defined as Hgb level below 8 mg dl,
- thrombocytopenia, defined as PLT <50,000 platelets per L,
- end-stage liver disease, and
- allergy

Antithrombotic medical dilemmas

Decisions to start effective AF-related stroke thromboprophylaxis following an acute ischaemic stroke or intracerebral haemorrhage are rarely clear-cut: patients have reluctance and own prejudices, and relative contraindications are influenced by their individual clinicians' perceptions of risks and benefits (5). It is therefore necessary to rigorously evaluate the current status of oral anticoagulation agent use for AF-related stroke prevention. Considering the difficulties involved in anticoagulant treatments, it is only reasonable to devise CEPDs (Cerebralembolic Protection Devices) capable of matching or surpassing current Warfarin/OAC efficacy.

1.3. What is the relation between TAVR and stroke?

TAVR has emerged as an alternative, rapidly evolving non-invasive procedure for patients with severe aortic stenosis and medium-to-high surgical risk. By 2025, there will be an estimated 280,000 TAVR procedures performed worldwide and the total market will exceed $8 billion. Although this highly promising treatment modality results in less morbidity, shorter time to recovery and similar mortality rates, it is still associated with one of the most devastating and feared complications: cerebral embolism, which in turn may cause stroke (17). Stroke is associated with a 6-fold increase in mortality in TAVR cohorts, a moderate to severe permanent disability in up to 40% of survivors (5), a 4.7-fold increased risk of permanent work disability (2), social isolation and significant financial strain in 80% of stroke survivors (13), and an increased risk of readmission in patients with stroke after cardiac catheterization (18).

The time in between the TAVR procedure and the cardioembolic event is an important factor when choosing stroke prevention treatments. Most of them occur in the acute phase following TAVR where cerebral embolic events are frequent (19). Nonetheless, according to the ADVANCE trial, half of the reported strokes occurred between day 2 and 30 after the TAVR procedure (20). Moreover, evidence is mounting on ischaemic brain lesions being produced after day 30, causing SBIs and long-term neurological symptoms. New ischaemic brain lesions were found in 74% to 100% of patients on diffusion-weighted magnetic resonance imaging (DW-MRI) after TAVR (21). Although studies have shown that SBI may not be related to apparent short-term neurological symptoms, evidence points to an association with accelerated cognitive decline and strengthening of the risk of long-term dementia (most commonly, Alzheimer's disease) (22). Later events are associated with patient specific factors (23). SBIs have been associated with accelerated cognitive decline and higher risk of long-term dementia. The situation is especially worrying given that TAVRs are being implanted in increasingly younger and lower risk patients, hence potentially increasing the prevalence of dementia.

1.4. What is the state of the art of cerebral protection devices?

As mentioned, in patients undergoing TAVR, stroke remains a potentially devastating complication associated with significant morbidity and mortality. This is especially worrying, given that TAVR is now indicated in aortic stenosis low- and intermediate-risk patients (24), and that stroke rate 30 days post-TAVR has been reported at 3.4% in low risk-patients (25). To prevent debris from embolizing to the brain during the procedure and reduce the risk of stroke, cerebroembolic protection devices (CEPDs) were developed (26). These devices are implanted during the procedure and up to 2 days after, since the clogging of CEPDs impedes them from being used to prevent ischaemic strokes >2 days post-TAVR. Nonetheless, as explained above, risk of stroke may not be limited to the procedure itself or the perioperative period. Moreover, the clinical benefit of current CEPDs in reducing strokes, transient ischaemic attacks or death remains unknown (27–29). It is therefore worrying that for strokes triggered by AF or other conditions extended in time, there are no currently approved CEPD in the market. The SENTINEL-LIR study demonstrated that embolic debris captured by the SENTINEL-CPS (Cerebral Protection System) during TAVR in low- to intermediate-risk patients was similar to that in previous studies conducted among higher-risk patients. These findings suggest lower-risk patients undergoing TAVR have potentially a similar embolic risk as high-risk patients, as evidenced by embolic debris capture (30). Most captured debris had a size of <500 m, with 78% between 150 and 500 m. Larger size particles ($\geq$1000 m), which can cause significant vessel obstruction, were present in 67% of cases. Therefore, the Sentinel CEPD can functionally capture large debris that may cause a

severe stroke. In contrast, debris on the micrometer scale may pass through the gaps between the filters and arteries, leading to stroke even in CEPD-protected territories (with less likelihood of severe symptoms) (31). Dedicated meta-analyses demonstrated that SBIs of small infarction volume 3 mm^3 are independent predictors of later stroke and mortality (18), further highlighting the need for a CEPD able to filter small debris in the long term post-TAVR. Such a device would be a radical improvement for a large population at risk.

1.5. How can this study help improve the current situation?

The main purpose of the work presented in this paper can be described with the simple motto: ***Save the brain***. The proposed solution consists of a stent filter/diverter attached to an electronegatively charged strut structure, intended to block the passage of clots or deflect their trajectories thanks to both fluid- and electro-dynamical forces on the clots. This can be achieved thanks to the electrostatic repulsion acting on naturally electronegatively charged blood clots, and its geometrical design, capable of filtering thrombi based on the distance between struts. The main objective of this device is to reduce or eliminate the percentage of blood clots entering the BCT, LCCA, and LSA, while maintaining at least 98% of the natural delivery of oxygenated blood to the brain. The Section **4.3** will demonstrate that the presence of the devices in all three arteries reduces the flowrate in a maximum of 7.5% in the case of BCT, and in less than 2% in the other two aortic arch arteries. This paper provides the details of the work carried out using Computational Fluid Dynamics (CFD) coupled with Lagrangian particle transport to validate the efficacy of the deflecting medical device positioned at the base of the BCT, LCCA, and LSA. A sufficiently large number of particles were injected into the domain in order to assure significant statistical samples for validating the particle-deflecting capabilities of the device. The study is divided in two main stages. The first one analyzes the effect of the thickness and shape of the strut design on the device performance. In the first stage, the purely hydrodynamic effect of the device is analyzed using a CFD and a particle transport model. The device is placed at the root of the LCCA and the optimal strut thickness is identified by analyzing the trajectories of particles suspended in the flow. The analysis showed a low efficacy for the deflection of thrombi and identified a deficiency in the initial design which is was not avoiding particles pass through the lateral struts. To overcome this deficiency, extra struts are added in the second design employed in the second stage of the work, oriented perpendicularly to the original struts. The second stage of this project, proposes to simulate struts that are electrically charged on their surface. Considering that blood clots are negatively charged, the strut surface would be negatively charged too in order to repel the clots. The proposed device consists of a stent NITINOL, plus Graphene oxide/ Bovine serum albumin nanoparticles (*Bovine serum albumin bioconjugated graphene oxide: Red blood cell adhesion and hemolysis studied by QCM-D .Bing Cai*) attached to an electronegatively charged strut, preventing the adhesion of cells and blood proteins, as well as reducing the possibility of hemolysis to minimal. The design is intended to block the passage of clots or deflect their trajectories being possible to deflect even the smallest particles more than 50% from entering the aortic arch arteries, offering a method for decrease Silent Brain Stroke. This can be achieved thanks to the electrostatic repulsion acting on naturally electronegatively charged blood clots, and its geometrical design, capable of filtering thrombi based on the distance between struts. The main objective of this device is to reduce or eliminate the percentage of blood clots entering the BCT, LCCA, and LSA, while maintaining at least 80% of the natural delivery of oxygenated blood to the brain.

The project has not yet been tested on animals or patients; these phases are planned for the future. Our initial prototype was developed to demonstrate proof of concept. The most recent design, which is nearing completion, is self-expanding and can be placed inside a 10-French catheter for delivery. In terms of deployment, CEPDs are implanted either during the procedure or up to two days afterward. After this period, the potential clogging of the CEPDs makes them unsuitable for preventing ischaemic strokes (>2 days post-TAVR). The risk of stroke may extend beyond just the procedure or perioperative period. One of the significant advantages of our Sentinel CEPD is its capability to capture large debris that could cause severe strokes. However, smaller debris on the micrometer scale might still bypass the filters, leading to potential strokes in CEPD-protected areas, albeit with a reduced chance of severe symptoms. Meta-analyses have indicated that small-volume SBIs (<3 mm^3) can predict subsequent strokes and increased mortality, underscoring the long-term need post-TAVR for a CEPD designed to filter out even small debris. Such a device would mark a significant advancement for a large at-risk population.

The effectiveness of CEPDs in minimizing strokes, transient ischemic attacks, or mortality remains to be determined (18). It's concerning when considering strokes induced by AF or other extended conditions.

For device residency duration, we should cater to two distinct populations: the elderly group with AF, or those immediately post-stroke to avoid anticoagulation. For both groups, the device would be permanently placed. For TAVI patients classified as low, medium, or high risk without AF, the device should remain for longer than 30 days, acting as a CPD, and based on their treating physician's discretion. However, for TAVI patients who either had AF before the procedure or developed it post-procedure, it's recommended to keep the device in place permanently.

2. Methods

2.1. Aortic arch geometry

The aortic arch geometry used for computational simulations was designed based on an anatomical model from a previous study (32). In order to adapt the geometry to the requirements of the present study,

some modifications were made using ANSA v22.1.0 (Beta Simulation Solutions, Lucerne, Switzerland). The applied modifications preserve the original structure of the aortic arch geometry, only in the LCCA and BCT significant changes (i.e., go from an anatomical structure to a synthetic one) have been applied. It was observed that the original geometry was not representative of an average BCT geometry, so it was manually corrected to adapt it to a more realistic one. Likewise, it was noticed that the LCCA presented a broader morphology at the entrance of the vessel, which could imply obtaining wrong conclusions, thus, it had to be corrected. Finally, let us comment that the aortic root was truncated to focus on the vessels in the aortic arch. For the inlet, the area corresponding to the left ventricle outflow tract (LVOT), with the coronary arteries and the aortic valve was replaced by a rigid tube to ensure the correct stabilization of the fluid. At the outlet, the area corresponding to the superior mesenteric, illiac, and renal arteries was dismissed. The resulting geometry used in this study can be observed in **Figure 1**.

For the second stage of the present work, the device is implanted at the base of the three arteries: BCT, LCCA, and LSA. **Figure 2** shows the patient-specific geometry of the aortic arch employed, with the arteries where the device will be placed. The inlet and outlet boundaries are labelled as:

- Inlet: Aortic root
- Outlets:
  - Brachiocephalic Trunk (BCT),
  - Left Carotid Common Artery (LCCA),
  - Left Subclavian Artery (LSA), and
  - Descending Aorta (DAO).

2.2. Device design

First stage

The emboli released from the aortic root due to TAVR-related debris tend to travel through the BCT, LCCA and LSA, obstructing the superior arteries and producing cerebral strokes, with the aforementioned associated consequences. Therefore, it is crucial that the introduced CEPD can be implanted in all three arteries of the aortic arch. The proposed solution, detailed in the patent no. US9517148 (33), fulfills exactly this requirement. It consists of a stent attached to a strut structure to block or deflect clot trajectories, as can be seen in **Figure 3**. This can be achieved thanks to its design, capable of filtering thrombi based on the distance between struts and eventually to modify trajectories of the smallest particles, responsible for SBI.

It is worth noting that the patent provides some flexibility in design parameters such as the strut orientation, convexity, profile, and quantity. The main application of this device is to reduce or eliminate the percentage of embolisms entering the BCT, LCCA and LSA in the mid- to long-term in AF and TAVR patients, while maintaining the delivery of oxygenated blood to the brain. The introduced device has the objective of reducing the number of particles travelling to the brain through the branches of the aortic arch. To do so, in the first part of the study, it is implanted at the base of LCCA. The choice to begin with this configuration takes into account different studies (34, 35) which suggest that cerebrovascular diseases, such as strokes, are significantly influenced by clots travelling through this artery.

The curved struts of the device are aligned with the aortic blood flow to effectively deflect particles from entering these vessels, without significantly reducing the fraction of ejected flow into the vessel where it is placed. The deflector structure has been designed with FreeCAD 0.19 (36) and merged to the aortic arch geometry with ANSA. For this step, both the dimensions stated in the reference study (37) and in the device patent have been considered. The deflector orientation angle with respect to the mean aortic flow was selected taking into account the results from (37). In this study, the centerline of the aortic arch has been taken as the direction for the deflector

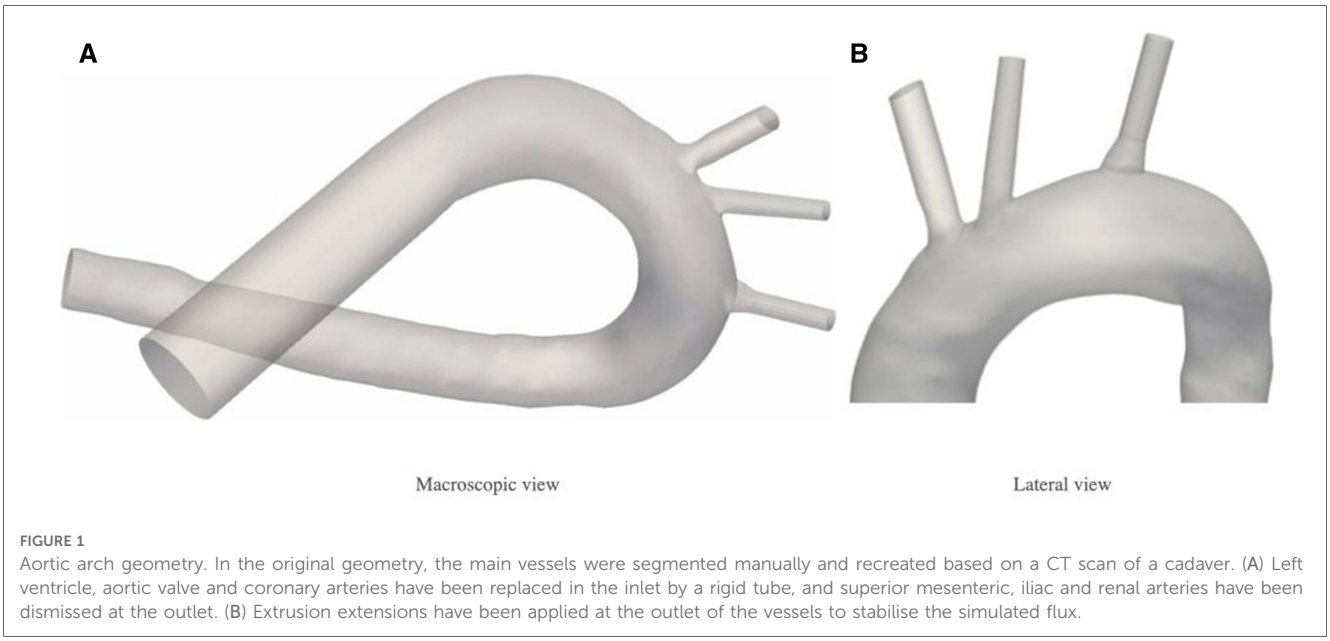

FIGURE 1
Aortic arch geometry. In the original geometry, the main vessels were segmented manually and recreated based on a CT scan of a cadaver. (**A**) Left ventricle, aortic valve and coronary arteries have been replaced in the inlet by a rigid tube, and superior mesenteric, iliac and renal arteries have been dismissed at the outlet. (**B**) Extrusion extensions have been applied at the outlet of the vessels to stabilise the simulated flux.

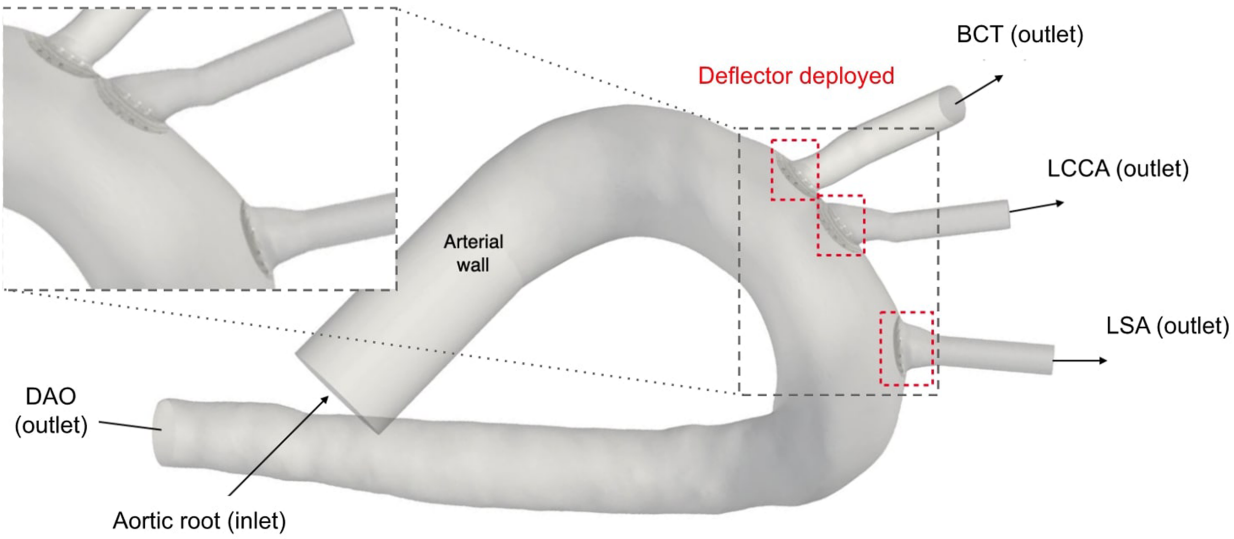

FIGURE 2
Geometry of the aortic arch and zoom-in of the deflectors deployed at all three arteries.

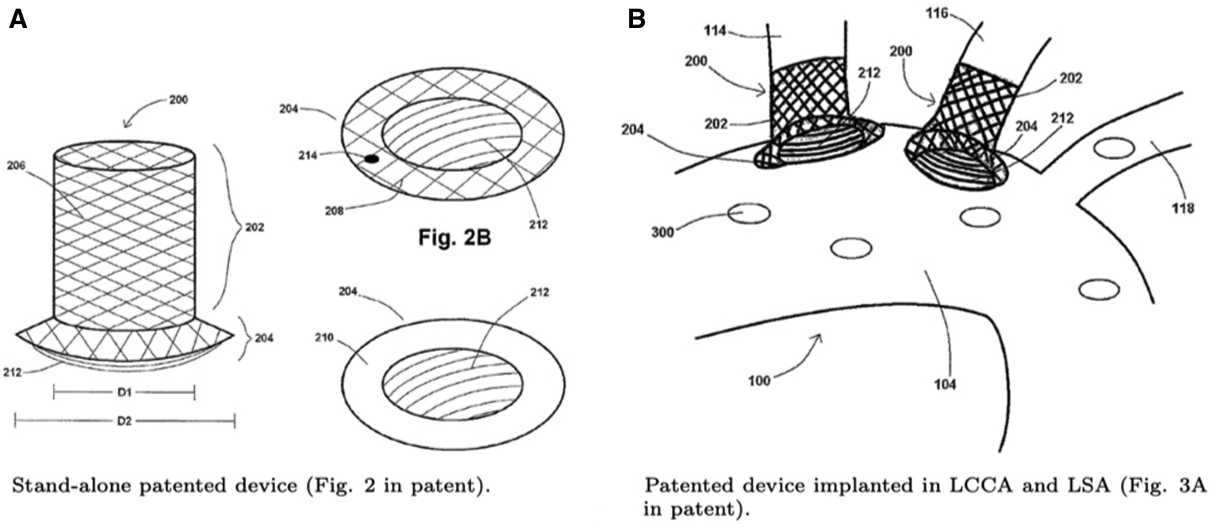

FIGURE 3
Diagrams from the patent of thrombus deflecting device, patent no. US9517148 (33).

positioning. Five different deflector geometries have been generated considering two geometric parameters: the distance between deflector struts or strut interval (L_{si}) and the strut thickness (L_{st}). Figure 4A shows the deflector design and the above mentioned parameters. The resulting geometry dimensions are illustrated in Table 1. Figure 4B shows the aforementioned deflector geometries.

Lateral spacing

An important factor that has to be considered in the construction of the geometry and the implantation of the device is the lateral free space between the first struts of the deflector and the wall of the artery. As shown in Figure 5, the space between the lateral strut and the device annulus at the base of the LCCA varies among geometries, corresponding to 2.17, 1.76, 2.76, 1.9 and 1.76 mm for the $L_{si} = 0.5, 0.75, 1.0, 1.25, 1.5$ mm devices respectively. That is, all geometries have a bigger lateral spacing than their corresponding L_{si}. The smaller lateral space of the $L_{si} = 0.75$ mm design with respect to designs with $L_{st} \in [0.5, 1.25]$ mm is consistent with the highest effectiveness in blocking particles from entering the LCCA as will be shown later in section "Results" for the first stage of the appendix provided in supplementary material. This is indicative of the critical impact of this geometric parameter in the design of the medical device.

Moreover, it is observed that some particles with larger diameter than the L_{si} of the device are able to enter the treated

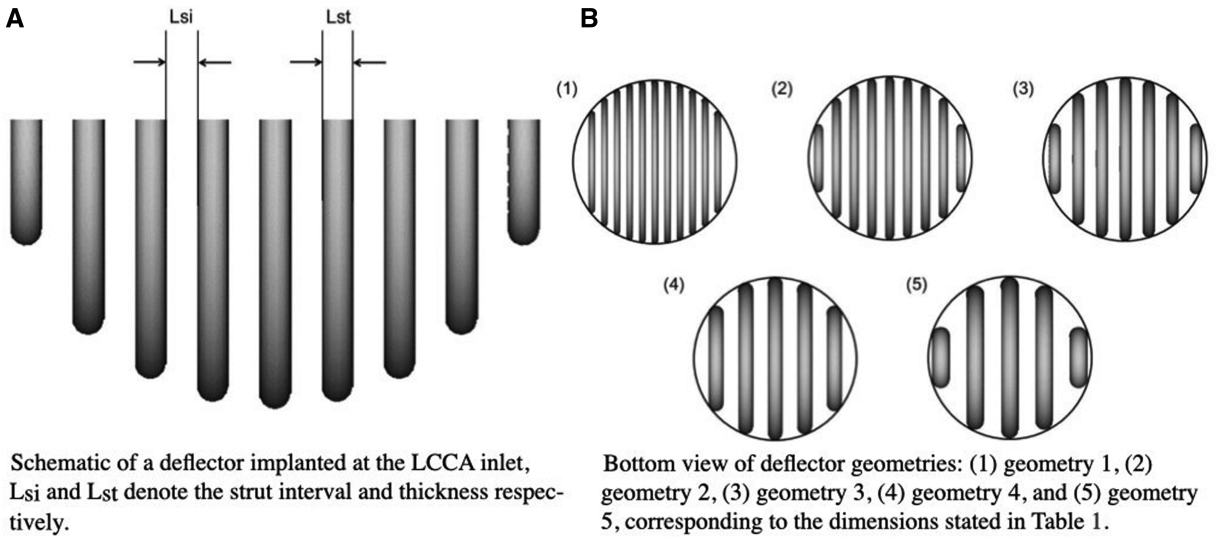

Schematic of a deflector implanted at the LCCA inlet, Lsi and Lst denote the strut interval and thickness respectively.

Bottom view of deflector geometries: (1) geometry 1, (2) geometry 2, (3) geometry 3, (4) geometry 4, and (5) geometry 5, corresponding to the dimensions stated in Table 1.

FIGURE 4
Schematics of device from different views.

TABLE 1 Dimensions for the design of the thrombus deflector for the different geometries generated.

Deflector geometry	L_{si} [mm]	L_{st} [mm]
Geometry 1	0.50	0.50
Geometry 2	0.75	0.75
Geometry 3	1.00	1.00
Geometry 4	1.25	1.25
Geometry 5	1.50	1.50

LCCA due to the above mentioned issue. Figure 6 shows a case where a large particle passes through the device and ends up in the LCCA. This extra lateral spacing explains the number of particles with diameter larger than L_{si} that get deposited in the LCCA output as well as the fluid jet that is also shown through this space in section: "Results" for the first stage of the appendix provided by the supplementary material.

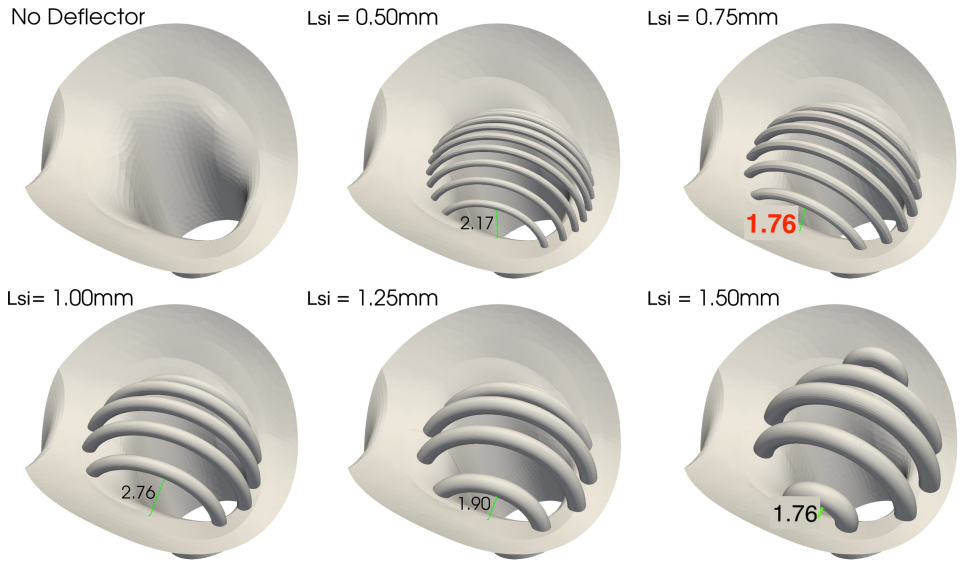

FIGURE 5
Deflector geometries of different strut thicknesses and inter-strut spacings. On top row from left to right: no deflector, $L_{si} = 0.5$ and 0.75 mm bottom row: $L_{si} = 1.0$, 1.25 and 1.5 mm. Spacings between lateral struts and annulus of base of LCCA are also displayed for each geometry. The $L_{si} = 0.75$ mm is of particular interest, since it is the most effective in blocking particles, with a lateral spacing of 1.76 mm as highlighted in red.

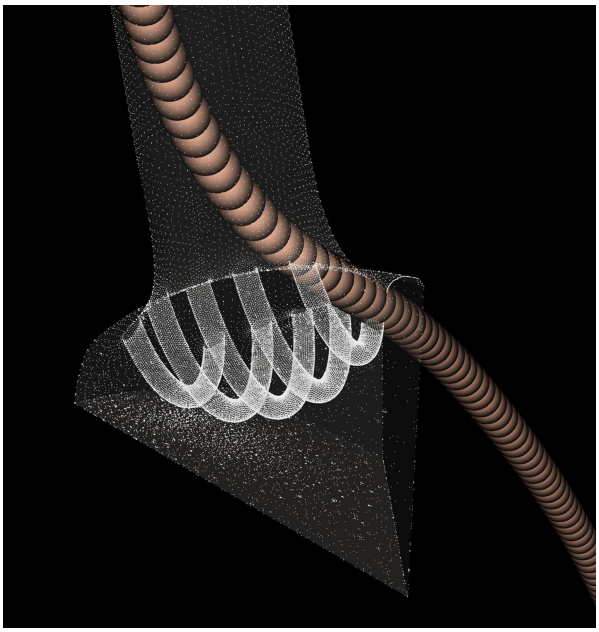

FIGURE 6
Particle with diameter larger than L_{si} passing through the device.

To overcome this deficiency, extra struts has been added in the new design employed in the second stage of the present work, oriented perpendicularly to the original struts, as it is shown in Figure 7.

Second stage

For the second stage of the present work, lateral struts were added to prevent particles from escaping through the side holes, the strut diameter was optimized and adapted to each of the three arteries.

Figure 7 shows the new struts added to the device to improve the particle filtering. It can be seen in this figure, that the strut thickness is not homogeneous, and instead thins out towards the ends (circled with red pointed lines). Note that this is an artefact of CAD model generation algorithm, in the creation of the 3D model, but is not a feature of the design or the patent involved. The thinning is an artefact of CAD model generation algorithm and in future versions of the design will be modified this morphology to maintain the section of the struts constant. Neither of the previous studies of this device had considered an electrical charge. In the second stage, electric charge is applied to additionally deflect small particles that could normally pass between the struts. The device would be covered with a negatively charged graphene oxide coating, with surface charges of -24000.0 statC cm^{-2}, which corresponds to the most extreme electrical charges found in the literature of biomedical devices, as will be described later in Section 9.1.2 (38).

3. Results

3.1. Particle deflecting efficacy

The subsequent results comes from the two stages of the presented work:

- For the first stage, with no electrical forces and as it has been described in Section 4.3 and illustrated in Figure 4B, the analysed particle deflecting efficacy is focused on the behaviour of the geometric design parameters: the distance between deflector struts or strut interval (L_{si}) and the strut thickness (L_{st}). The deflector is only located at one artery, LCCA, and 5 different prototypes based on mentioned parameters are analysed and presented in the Supplementary Appendix.
- The second stage of the work, now with electrical forces computed, covers the effect of multiple devices deployed at the same time. In

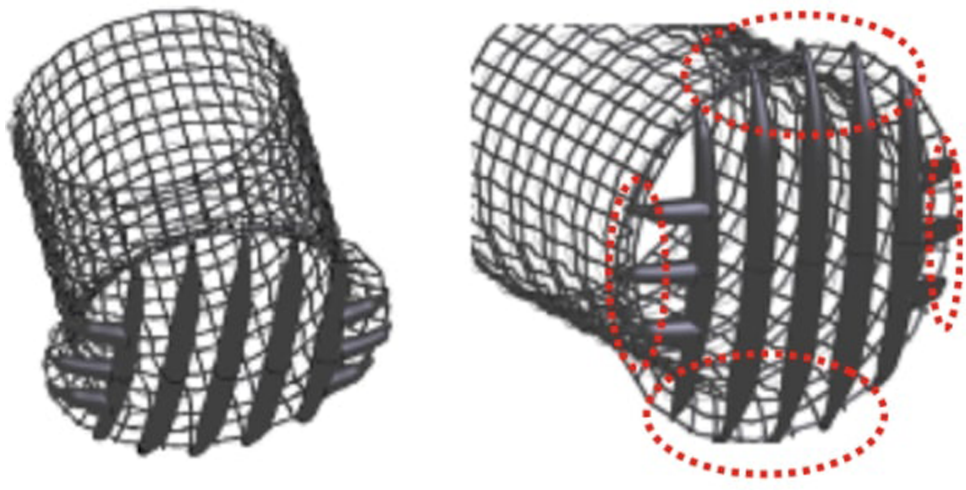

FIGURE 7
New deflector design. Lateral struts added are circled in red.

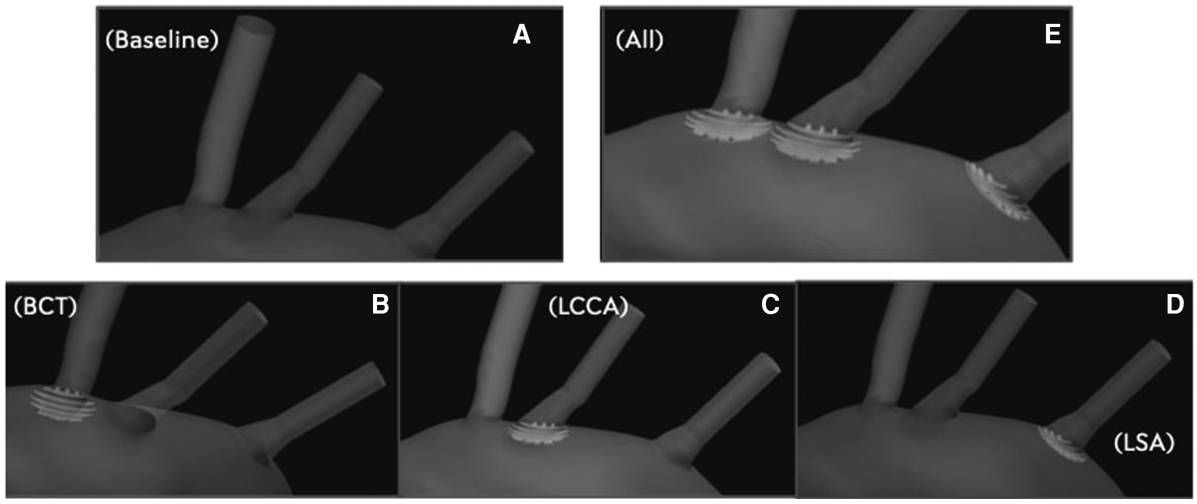

FIGURE 8
Five different device deployment configurations: (A) no deflector, (B) only in BCT, (C) only in LCCA, (D) only in LSA, (E) in 3 arteries.

particular five different device deployment configurations shown in Figure 8 are presented, which corresponds from non-deflector (8A) case to deflector located in all 3 arteries (8E), considering also the singles cases, this means deploying a single deflector at the base of the BCT only (8B), at the base of the LCCA only (8C) and at the base of the LSA only (8D). All of these also consider the effect of the electric field produced when the device is recovered by an electrically material. For each case, a total of 6 million particles were injected into the domain during the full length of each simulation. This ensemble of particles is equally distributed among 10 different particle types, that is, injecting 150,000 particles of each type during the full length of each simulation. The 10 particle types are a result of the combination of 5 particle sizes and 2 electrical charge conditions. The particle injections are distributed in time, with 3 injections per cardiac cycle. In each injection, 10,000 particles of each type were introduced into the inlet, homogeneously distributed in space. The 5 different particle diameters considered here are the ones presented in Table 4 except the last two, that has been avoided now due to the dimensions of the chosen configuration in the previous stage.

3.1.1. Healthy patient

Comparison between electric field repulsion and no-charged device for the optimum configuration of first stage

In this second stage of the work, as it is described below, 10 simulations are carried out. In each of one, for each size of the particles, 2 electrical charge conditions were considered: neutral and electrically charged. The thrombus deflecting performance of the electrically charged device was evaluated with a flow rate waveform representative of a healthy patient (see Figure 12A). This waveform corresponds to a heart rate of 70 bpm and a cardiac output of 4.286 L min^{-1}. As a baseline, the simulation was first run without deploying the deflector (Figure 8A), recording the number of particles of each type exiting each arterial outlet of the domain. Then, the device was deployed individually in each one of the 3 aortic arch arteries, repeating the process (Figures 8B–D), with particle filtering efficacies shown in Table 2a. Finally, the device was deployed in all 3 aortic arch arteries simultaneously (Figure 8E), with the particle filtering efficacies shown in Table 2b. The absolute number of particles of each type exiting each artery were recorded and are given in Table 6a of the appendix.

When the deflector is implanted in a single artery, it effectively reduces the number of particles there, producing increases in the untreated arteries (Table 2a). Moreover, the filtering effect is improved when the electrical charge is considered. When deploying the device in all arteries, the number of particles are also reduced in all terminals, on average by 62.6%, but it is necessary to consider the electrical charge in order to produce the desired effect (Table 2b).

3.1.2. Atrial fibrillation patient

Comparison between electric field repulsion and no-charged device for the optimum configuration of first stage

In a second step, a flow rate waveform representative of an AF patient was imposed at the inlet. This waveform corresponds to a heart rate of 150 bpm and a cardiac output of 3.429 L min^{-1}, which corresponds to a 20% decrease with respect to the healthy patient (39). As for the previous section, the five deployment setups shown in Figure 8 were considered: baseline (no deflector), deploying the device only in the BCT, only in the LCCA, only in the LSA, and in all three arteries simultaneously. The particle filtering efficacies for the deflector deployed in single arteries are shown in Table 3a, while Table 3b gives the efficacies for the deflector deployed in all arteries at once. The absolute particle counts in each artery are shown in Table 7a of the appendix.

As observed for the healthy patient, in the diseased patient deploying the deflector in single arteries filters particles, even

TABLE 2 Particle filtering efficacies for healthy patients.

Device position	Particle diameter	BCT		LCCA		LSA	
		Neutral	Charged	Neutral	Charged	Neutral	Charged
BCT	10 μm	1.1%	73.3%	-2.1%	-14.3%	7.0%	1.6%
BCT	50 μm	1.1%	56.5%	-2.3%	-15.6%	7.1%	2.7%
BCT	100 μm	1.6%	41.5%	-2.5%	-13.8%	7.5%	3.1%
BCT	500 μm	17.8%	30.0%	-19.2%	-18.7%	-1.3%	-16.9%
BCT	1 mm	100.0%	100.0%	-295.3%	-289.0%	-26.0%	-43.6%
LCCA	10 μm	-6.3%	-10.5%	4.4%	95.5%	16.5%	17.1%
LCCA	50 μm	-6.2%	-10.9%	4.4%	79.7%	16.5%	13.9%
LCCA	100 μm	-6.2%	-18.1%	4.9%	61.2%	16.5%	12.9%
LCCA	500 μm	-4.0%	-5.0%	19.7%	36.2%	-16.6%	-32.1%
LCCA	1 mm	-0.9%	-0.9%	100.0%	100.0%	-287.1%	-303.5%
LSA	10 μm	-17.3%	-17.2%	-17.6%	-17.9%	11.7%	92.5%
LSA	50 μm	-17.2%	-17.2%	-18.1%	-18.3%	11.8%	76.5%
LSA	100 μm	-17.1%	-17.1%	-17.9%	-17.9%	11.3%	50.0%
LSA	500 μm	-16.9%	-16.9%	-17.6%	-17.6%	-0.6%	4.0%
LSA	1 mm	-13.0%	-13.0%	-14.4%	-14.2%	100.0%	100.0%

(a) Particle filtering efficacies for the healthy patient deploying the device in single arteries (BCT, LCCA, or LSA), computed with respect to the baseline configuration. Columns correspond to the artery where particles are counted, and whether the particle is neutral or charged. Rows correspond to where the deflector is deployed, and particle sizes. When the efficacy is positive (i.e., number of particles is reduced), cells are painted in green. Otherwise, they are painted in red.

Particle diameter	BCT		LCCA		LSA	
	Neutral	Charged	Neutral	Charged	Neutral	Charged
10 μm	-0.9%	69.7%	4.7%	94.4%	21.2%	92.7%
50 μm	-0.9%	52.9%	4.6%	75.8%	21.2%	79.4%
100 μm	-0.5%	36.6%	4.8%	50.7%	20.8%	54.6%
500 μm	17.1%	28.7%	-0.7%	16.9%	-14.5%	-12.8%
1 mm	100.0%	100.0%	100.0%	100.0%	100.0%	100.0%

(b) Particle filtering efficacies for the healthy patient deploying the device in all arteries (BCT, LCCA, and LSA), computed with respect to the baseline configuration. Columns correspond to the artery where particles are counted, and whether the particle is neutral or charged. Rows correspond to the particle sizes. When the efficacy is positive (i.e., number of particles is reduced), cells are painted in green. Otherwise, they are painted in red.

without considering electrical charge (see Table 3a). Nonetheless, only significant particle filtering efficacies (between 21.2% and 100%) are observed when the electrical charge is activated. As seen for the healthy patient, this has the collateral effect of increasing the particle counts in the untreated arteries. On the other hand, when deploying the deflectors in all arteries at once, the electrical charge is necessarily required to filter out particles, with an average efficacy of 51.2% (see Table 3b).

4. Discussion

4.1. Device efficacy in the healthy patient

In this section the device performance is analyzed for the healthy flow rate conditions, in the baseline (i.e., no deflector), deploying a single deflector on each one of the aortic arch arteries separately, and finally deploying the deflectors in all arteries at once.

TABLE 3 Particle filtering efficacies for the AF patient.

Device position	Particle diameter	BCT		LCCA		LSA	
		Neutral	Charged	Neutral	Charged	Neutral	Charged
BCT	10 µm	10.5%	63.1%	-18.1%	-26.6%	-15.3%	-18.6%
BCT	50 µm	10.6%	46.3%	-18.3%	-27.6%	-15.0%	-18.0%
BCT	100 µm	10.9%	35.9%	-18.8%	-27.7%	-14.3%	-17.2%
BCT	500 µm	15.9%	21.2%	-24.4%	-24.1%	13.5%	7.2%
BCT	1 mm	100.0%	100.0%	-328.5%	-327.2%	13.0%	4.0%
LCCA	10 µm	-9.9%	-13.8%	4.0%	76.5%	18.9%	16.8%
LCCA	50 µm	-10.1%	-20.4%	4.8%	55.3%	18.7%	15.2%
LCCA	100 µm	-10.8%	-26.5%	8.0%	45.2%	16.9%	14.2%
LCCA	500 µm	-2.2%	-3.6%	42.0%	46.3%	-18.4%	-20.7%
LCCA	1 mm	-0.2%	-0.8%	100.0%	100.0%	-169.4%	-174.2%
LSA	10 µm	-9.7%	-9.7%	-6.9%	-6.8%	16.2%	79.8%
LSA	50 µm	-10.0%	-10.0%	-6.3%	-6.2%	17.1%	60.3%
LSA	100 µm	-9.4%	-10.2%	-5.6%	-5.7%	18.0%	38.6%
LSA	500 µm	-9.4%	-9.4%	11.1%	11.2%	22.8%	25.9%
LSA	1 mm	-5.8%	-5.8%	7.0%	6.9%	100.0%	100.0%

(a) Particle filtering efficacies for the AF patient deploying the device in single arteries (BCT, LCCA, or LSA), computed with respect to the baseline configuration. Columns correspond to the artery where particles are counted, and whether the particle is neutral or charged. Rows correspond to where the deflector is deployed, and particle sizes. When the efficacy is positive (i.e., number of particles is reduced), cells are painted in green. Otherwise, they are painted in red.

Particle diameter	BCT		LCCA		LSA	
	Neutral	Charged	Neutral	Charged	Neutral	Charged
10 µm	-6.0%	54.4%	-4.2%	73.5%	11.7%	80.8%
50 µm	-5.0%	31.7%	-4.4%	43.6%	12.3%	61.8%
100 µm	-5.1%	10.0%	-2.1%	25.9%	12.7%	41.1%
500 µm	17.3%	20.1%	13.7%	20.1%	2.9%	4.9%
1 mm	100.0%	100.0%	100.0%	100.0%	100.0%	100.0%

(b) Particle filtering efficacies for the AF patient deploying the device in all arteries (BCT, LCCA, and LSA), computed with respect to the baseline configuration. Columns correspond to the artery where particles are counted, and whether the particle is neutral or charged. Rows correspond to the particle sizes. When the efficacy is positive (i.e., number of particles is reduced), cells are painted in green. Otherwise, they are painted in red.

4.1.1. Baseline: no deflector

In the baseline configuration, that is without any deflector deployed (Figure 8A), it can be observed in Figure 9 that for the smallest particles (10–100 m), the number of particles exiting each outlet is inversely related to the proximal distance to the aortic root (in increasing order: BCT, LCCA, LSA, and DAO). This tendency is reversed for the largest particles (500 m to 1 mm), for which the number of particles at each outlet increases with the proximal distance instead. This observation can be explained by the fact that as the particles get larger, their inertia dominates over the flow advection, resisting to curve their trajectory, and thus entering the first outlet that they encounter along their straight path. On the other end, smaller particles are dominated by the flow advection, and thus are more evenly

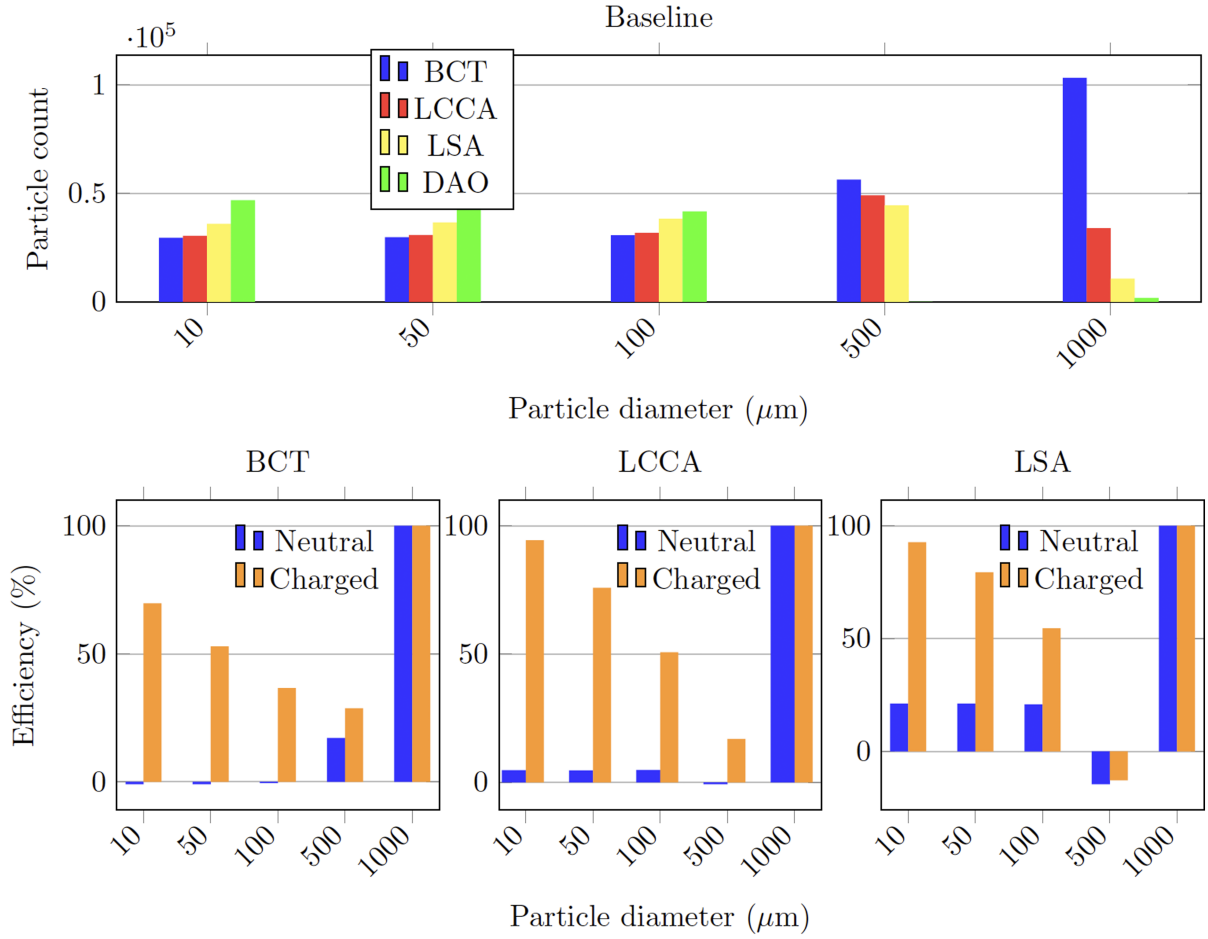

FIGURE 9
Particle counts of the healthy patient with deflector positioned at all arteries.

distributed between the outlets, with most particles exiting the widest outlet, the DAO.

4.1.2. Deflector deployed in a single artery

Following the baseline case, the deflector was deployed individually in each aortic arch artery (BCT, LCCA, or LSA), running separate simulations for each case (**Figures 8B–D** respectively). These setups are intended to isolate the effect of the deflector on each artery and to quantify the collateral effect on the complementary arteries. Here, the complementary arteries refers to the arteries left untreated (e.g., BCT and LSA), when the deflector is deployed in a given artery (e.g., LCCA). A significant reduction in the particle counts is observed for the treated arteries (thick borders in **Table 2a**), from the neutral particles to their charged counterparts. Five main observations are noted with respect to this effect:

1. the neutral particles are filtered with an efficacy of 26% on average in the artery where the deflector is deployed,
2. this average efficacy increases to 66.5% when the particles are charged,
3. the deflection efficacy of the electrical charge diminishes for larger particle sizes,
4. the number of particle counts of arteries distal to the artery where the deflector is deployed increase by 38.8% on average with respect to the baseline case (no deflector), and
5. they increase to 46.6% when the particles are electrically charged.

Regarding the third point, the deflection of particles is most effective for the smallest particles (10 m), which reduce their counts by 73.3%, 95.5%, and 92.5% at the BCT, LCCA, and LSA, when deploying the deflector in each one of these arteries respectively. Note that this effect is observed for all particle sizes, except for the largest (1 mm), which are directly filtered because they can't fit in between the struts, and exit through the DAO instead. Regarding the second and third observations listed above, it can be seen in **Table 2a** that deploying the deflector in a given artery increases the number of particles in the free distal arteries by 38.8% on average, while only increasing the particle counts by 12.7% in the proximal arteries. This effect is enhanced when the particles are electrically charged, further increasing particle counts by 46.4% in the distal arteries, and 14.2% in the proximal arteries. The fact that deploying the deflector in a single artery may have negative consequences in either of the

remaining aortic arch arteries, motivates the deployment of the device in all three arteries, as described in the following section.

4.1.3. Deflectors deployed in all three arteries

Three deflectors were deployed in all arteries (BCT, LCCA, and LSA) simultaneously, imposing the healthy patient flow rate curve at the inlet. This setup is intended to fully protect the cerebrovascular circulatory system from cardioembolisms coming from the aortic root. **Table 2b** shows the corresponding particle counts in each one of the arterial outlets, which are plotted in **Figures 9** for the BCT, LCCA, and LSA respectively. Electrically charging the device struts reduces the number of particles entering the aortic arch arteries in all cases, except for the largest particles (1 mm), which are blocked with or without charge, since they can't physically fit between the struts (the inter-strut spacing is 0.75 mm). On the other end of the size spectrum, as for the treated arteries in section corresponding on the single artery study, the electrical deflection mechanism is strongest for the smallest particles (10 m), and is diminished as the particles get larger and inertia increasingly dominates over electrostatic forces. Interestingly, except for the 500 m particles, the device has a two-fold deflecting/filtering mechanism: while the smallest particles are deflected by electrostatic repulsion (>50%), the largest ones are mechanically filtered since their diameter is similar or larger than the inter-strut spacing (100%). In consequence, the device effectively avoids a wide range of particle sizes from entering the aortic arch arteries, protecting the cerebrovascular system. For the 500 m particles, the effect of the device located in all three arteries leads to a unexpected behavior in the LSA, where it actually increases the number of particles entering the artery (**Figure 9**). This issue must be addressed in further detail in future iterations. It is nonethelesss worth mentioning that the effect of the electric field attenuates the problem presented in this case.

4.2. Device efficacy in atrial fibrillation patient

In this section the device efficacy is analyzed for the AF flow rate conditions, in the baseline (no deflector, **Figure 8A**), deploying a single deflector on each one of the aortic arch arteries separately (**Figures 8B–D**), and finally deploying the deflectors in all arteries at once (**Figure 8E**).

4.2.1. Baseline: no deflector

As for previous section, the baseline configuration is examined for the AF case, that is without any deflector deployed (**Figure 8A**). As for the healthy patient, **Figure 10** shows that the particle counts for the smallest particles (10–100 m) are inversely related to the proximal distance to the aortic root. For the larger particles (500 m to 1 mm), the inverse tendency which was observed for the healthy patient, is also observed in the AF patient in **Figure 10**. The fact that the behaviour is conserved, indicates that the tendencies in final particle positions are maintained from the healthy to the diseased patient, in a statistical sense.

4.2.2. Deflectors deployed in all three arteries

When deploying the deflector in all three arteries in the AF conditions, similar results are observed to those seen in the analogous case of healthy patient. **Table 3b** shows the corresponding particle counts in each one of the arterial outlets, which are plotted in **Figures 10** for the BCT, LCCA, and LSA respectively. This is, the deflector effectively reduces the number of neutral particles entering the treated aortic arch arteries, by 22.9% on average. When the electrical charge is incorporated, the filtering efficacy further increases, to 51.2%. As in previous sections, the largest particles (m) are blocked with or without charge, since they can't physically fit between the struts (the inter-strut spacing is 0.75 mm). Therefore, once again the two-fold deflecting/filtering mechanism of the device is evidenced: while the smallest particles are deflected by electrostatic repulsion, the largest ones are mechanically filtered since their diameter is similar or larger than the inter-strut spacing.

4.3. Device safety

One of the main necessary conditions to assure the safety of the device, is that the presence of the deflectors does not reduce the blood flow rate significantly into the aortic arch arteries, necessary to provide the brain with oxygenated blood. **Figure 11** overlap the flowrate curves at these arteries, in the baseline case (without deflector) and in the case where the three devices are deployed simultaneously, both for the healthy and AF patients. These correspond to the worst case scenarios for reduction of the flow, and therefore are sufficient to assure the device safety when the device is deployed in a single or two arteries. From these curves, it is observed that the device does not alter the flow rates significantly in any case. The maximum reduction is found in the BCT artery, with a 8.63% reduction for AF patients and 8.64% for healthy ones, with respect to the baseline case. In the LCCA artery the reduction is equal to 1.61% and 1.59% for AF and healthy patients while for LSA there is 4.03% and 3.97% less flow for the AF and healthy patients respectively when the device is deployed. In summary, the model predicts that the device reduces the ejected flowrate to the aortic arch arteries by significantly less than 20%, which is the maximum tolerated physiological reduction. Therefore, the device complies with the necessary condition set at the beginning of this report, which is required to assure a healthy cerebrovascular function of the treated patient.

4.4. Clogging of the device

Particles blocked by the mere fact that their diameter is larger than the inter-strut spacing may cause concern regarding clogging of the device, as occurs with conventional CEPD. The current numerical model cannot evaluate this aspect since deformability of the particles is not modelled. Nonetheless, it is somewhat reassuring that in contrast to conventional CEPD, the current device has a positive convexity which slightly bulges into the main aortic domain. This geometric attribute combined with the high velocities in the aorta result lower the possibility of particles getting stuck in between struts.

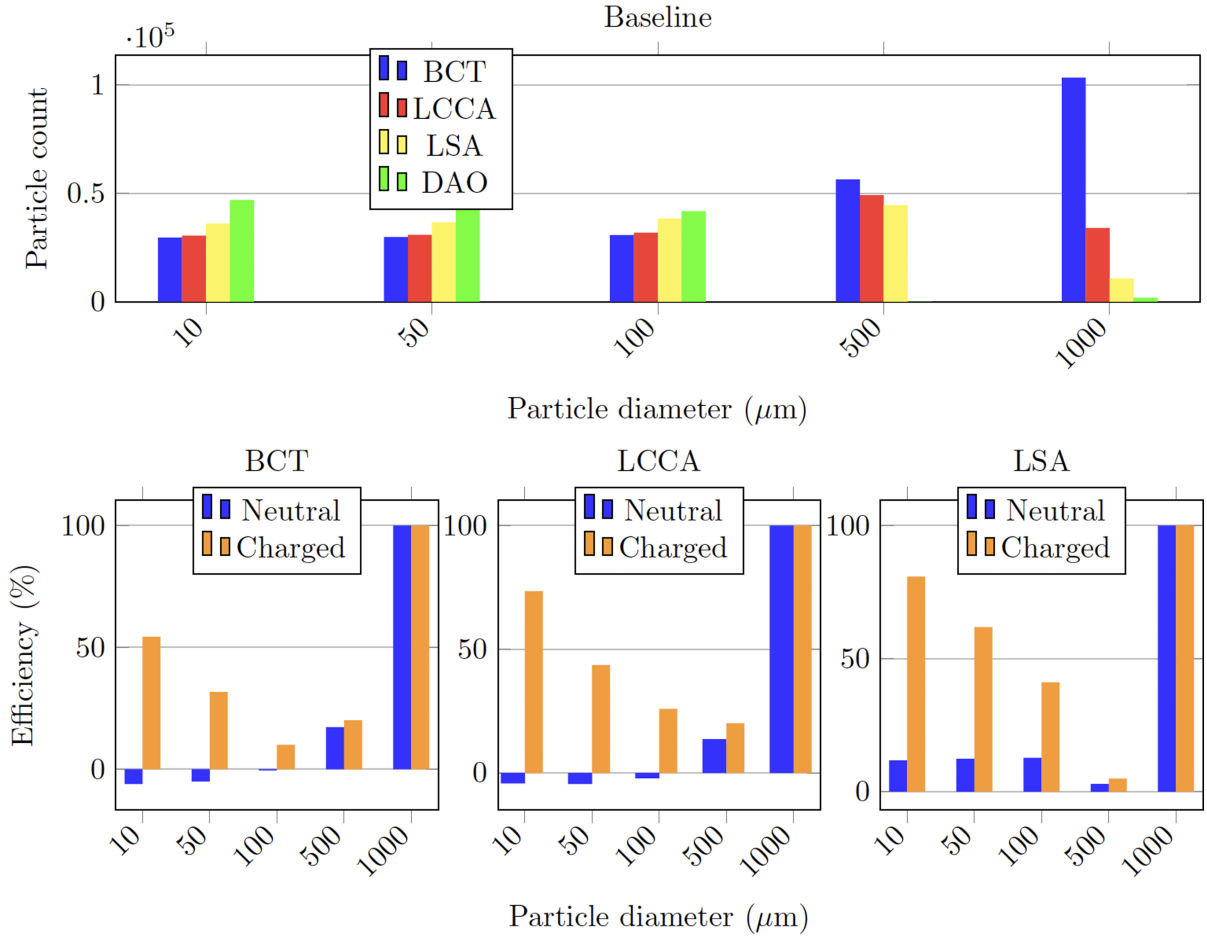

FIGURE 10
Particle counts of the AF patient with deflector positioned at all arteries.

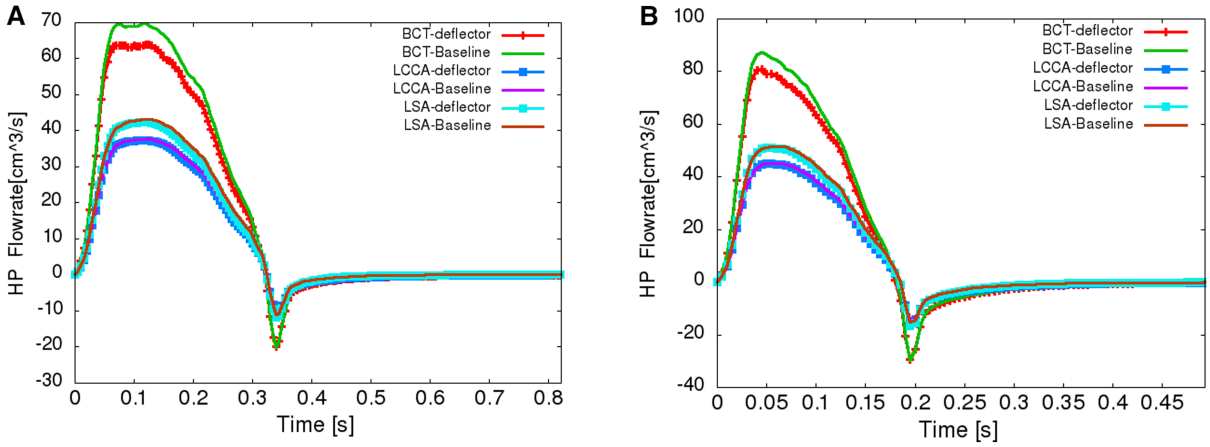

Blood flow rates at outlets in the healthy patient, not significantly altered by the presence of the deflector.

Blood flow rates at outlets in the AF patient, not significantly altered by the presence of the deflector either.

FIGURE 11
Safety flowrates. Reduction of the blood flow rate not significantly into the aortic arch arteries. (A) Blood flow rates at outlets in the healthy patient, not significantly altered by the presence of the deflector. (B) Blood flow rates at outlets in the AF patient, not significantly altered by the presence of the deflector either.

This effect is also addressed and improved introducing the repulsive electrical force due to the inverse distance proportional factor presented in this force.

5. Limitations

One of the limitations in the mathematical model considered is to assume clots as point-like particles for the fluid-particle interaction. As it was described in section "Thrombus model: particle transport" of the appendix provided in the supplementary material, the tracking is obtained by integrating the second Newton's law, so, mass affects in the effect of the forces but not shape. Moreover, the fluid-particle coupling is one-way, that is, particles do not influence the fluid flow. These two approximations are not accurate for particles well above the Kolmogorov scale of the flow. Therefore, errors introduced by the point-like approximation can be seen to increase with particle size. For the collisions of particles with the domain walls, particles were modelled as perfect spheres, and slip boundary conditions were imposed. The rigidity and shape of spherical particles may introduce further errors in the model when compared to blood clots which are deformable and amorphous. The slip boundary conditions have shown more realistic results than considering boundary conditions, but still do not fully reproduce the interaction of blood clots with the aortic lumen, which could be improved.

In addition to limitations in the mathematical model, the physical parameters used in the present work are based on the scarce references found in literature, of limited credibility. Therefore, to assure a higher credibility of the results, these parameters require further verification and validation with experimental data. Some examples of these parameters that are complex to determine, are the permittivity of the blood, the electric charge and diameters of the clots, and the charge of the strut graphene oxide coating. Moreover, it is necessary to clearly determine the physiological limits for the device electrostatic charge, strong enough to produce a significant effect on particles, but not so strong so as to onset hemolysis or cause negative physiological consequences.

Regarding the geometrical model of the device, due to an artefact introduced in the CAD generation, the side struts were modelled with a heterogeneous thickness, thinning out towards the ends. This implies that free space greater than 1 milimeter is found in the device. This feature is hypothesized to have produced the spurious effect of actually increasing the number of 500 m particles entering the treated LSA in the healthy case. This is, nonetheless, a model that will be evaluated and improved in further phases. The present study is a proof of concept that demonstrates the potential of the proposed device and the methodology to be optimized, but, given the novelty and risk of the proposed device, it is imperative to carry out a thorough experimental validation.

6. Conclusions

The present study carry out a computational analysis of a thrombus diverting and filtering device, designed as a solution to stroke and SBIs, critical health issues which are becoming more frequent given aging populations, increasing prevalence of AF, and devices being deployed in increasingly younger patients. The work has been carried out in two main stages. The first one analyzed the effect of the thickness and shape of the strut design on the device performance. The purely hydrodynamic effect of the device was analyzed using a CFD and particle transport model. The device was placed at the root of the LCCA and the optimal strut thickness was identified by analyzing the trajectories of particles suspended in the flow.

In the second phase, given the electronegative charge of blood clots, a negative electrostatic charge is imposed on the deflector struts in the device design, in order to repel thrombi. The computational model employed for this analysis combines computational fluid dynamics and electrostatics. The numerical analysis results showed that, while maintaining the patient models' blood flow at healthy levels, the introduced electronegatively charged device filtered particles of a wide range of sizes (10 m to 1 mm) from entering the aortic arch arteries, and with a higher efficacy than for the previous uncharged device. Moreover, the range of filtered particle sizes may be wider than for the only FDA-approved cerebroembolic protection device, the SENTINEL Cerebral Protection System, which has been shown to mainly capture debris of sizes <500 m (40). In the SENTINEL-LIR STUDY (30) larger size particles(>1000 m) which can cause significant vessel obstruction were presen in 67% of cases.Therefore, the results presented encourage the continuation of the development of this device.

The analysis has been conducted on two different patient conditions, healthy and diseased (i.e., suffering from atrial fibrillation) and five different particle sizes have been considered, ranging from 10 m to 1 mm. A balance was observed between the electrostatic, drag, and inertial forces acting on particles. The particle size was observed to determine which force dominates the particle dynamics. Given the numerical parameters employed in this study, the electrostatic force presents the strongest deflection effect on the smallest particles (10–50 m), which are most effectively diverted by the device. On the other end of the spectrum (500 m to 1 mm), the electric field cannot overcome the drag and inertial forces, which govern the larger particles' trajectories, but are mechanically filtered since they cannot fit within the struts. In summary, while the smallest particles are deflected by electrostatic repulsion, the largest ones are mechanically filtered. Therefore, the proposed design effectively blocks all the range of particle sizes analyzed in this study, offering an anticoagulant-free method to prevent stroke (particles¿1mm) and decrease small particles SBIs cause, especially useful given the growing population of elderly and AF patients. In particular, the results showed that when the device is placed in all three aortic arch arteries, the number of particles entering these arteries was reduced on average by 62.6% and 51.2%, for the healthy and diseased models respectively, matching current oral anticoagulant efficacies. The higher filtering efficiency shown for smallest particles, around 95%, may help prevent microembolisms, associated with accelerated cognitive decline and higher risk of long-term dementia, while larger particles >0,75, 1, 2 mm or more, the efficiency of the filter (100%) avoid the occlusion larger diametercerebral vessels causing severe stroke episode. Theoretically in elderly patients with AF, anticoagulant

therapy could not be used, with the great advantages that this means subsequent randomized and multicenter clinical trials are necessary to confirm this exciting and provocative new hypothesis.

7. Future work

The present study presents a methodology to model the problem of interest, and, assuming the considered range of parameters to be physiologic, shows preliminary evidence of the efficacy of the device for thrombus deflection. Nonetheless, further studies will be carried out to improve the solution, verify, and validate the model, validate the ranges of physical parameters employed, and refine the geometrical design for the target application. The scope of the current study was to quantify the efficacy of thrombus deflection by comparing the geometries without deflector vs. with deflector in the three arteries of the aortic arch. This has left the study of other aspects outside the scope of this work. The following are some of the aspects which will be studied in further detail in order to optimize the device design and exhaustively characterize its performance:

- Refine the number of intermediate particle sizes evaluated, between 50 to 500 m, to determine the critical diameter at which the flow forces dominate over the electrostatic repulsion.
- Guarantee that the parameters employed are within ranges that can assure a sufficiently low patient risk.
- Test the device on heterogeneous populations of virtual patients, that represent real-world diversity, regarding age, sex, and comorbidities.
- Test the electrostatically charged deflector in geometries with different distributions and convexities, respecting the original design of the reference patent (33).
- Based on the presented device, a novel one piece design would enable the easy retrieval in TAVR patients 30–40 days post-procedure, where in contrast, the design analyzed in the current work, composed of 3 separate deflectors, could be focused on the treatment of elderly patients. The one piece design will be modeled and tested in future iterations.

Data availability statement

The original contributions presented in the study are included in the article/**Supplementary Material**, further inquiries can be directed to the corresponding author.

Author contributions

JN conceived of the presented idea. MV contributed to the design and implementation of the research. CB and MF carried out the construction of all the meshes. BE and DO set the inputs of the simulation and MF and AC performed the computations. GH contributed to all the computational framework issues giving his valuable support on all the related questions. BE, with his help, implemented the new features to address the presented work in the in-house code developed in the department of her institution. AC carried out the bibliography research to set the numerical parameters of the electrical properties of the problem. DO, MF, and AC created the tables of results. MV and JN supervised the findings of this work. BE took the lead in writing the manuscript. All authors provided critical feedback and helped shape the research, analysis and manuscript. All authors contributed to the article and approved the submitted version.

Acknowledgments

This research has been supported by "ELEM biotech - the virtual human factory" (www.elem.bio), an INPhINIT fellowship from "la Caixa" Foundation (fellowship ID: LCF/BQ/DI18/11660044), by the European Union's Horizon 2020 research and innovation program under the Marie Sklodowska-Curie grant agreement No. 713673., by the project CompBioMed2 (H2020-EU.1.4.1.3. Grant No. 823712), by CREXDATA project (HORIZON-CL4-2022-DATA-01. Grant No. 101092749) and by Torres Quevedo Program (PTQ2018-010290), Ministerio de Ciencia e Innovacion, Spain. ELEM Biotech was not involved in the study design, analysis, interpretation of data, the writing of this article or the decision to submit it for publication.

Conflict of interest

DO, MF, ACM and MV are employed by ELEM Biotech. MV is an investor of ELEM Biotech.

The remaining authors declare that the research was conducted in the absence of any commercial or financial relationships that could be construed as a potential conflict of interest.

Publisher's note

Supplementary material

The Supplementary Material for this article can be found online at: https://www.frontiersin.org/articles/10.3389/fcvm.2023.1233712/full#supplementary-material

References

1. Donkor E. Stroke in the 21st century: a snapshot of the burden, epidemiology, quality of life. *Stroke Res Treat*. (2018) 2018:1–10. doi: 10.1155/2018/3238165

2. Blackshear JL, Odell JA. Appendage obliteration to reduce stroke in cardiac surgical patients with atrial fibrillation. *Ann Thorac Surg*. (1996) 61(2):755–9. doi: 10.1016/0003-4975(95)00887-X

3. Babu CS, Sharma V. Two common trunks arising from arch of aorta: case report and literature review of a very rare variation. *J Clin Diagn Res*. (2015) 9(7): AD05–AD07. doi: 10.7860/JCDR/2015/14219.6253

4. Pastori D, Menichelli D, Gingis R, Pignatelli P, Violi F. Tailored practical management of patients with atrial fibrillation: a risk factor-based approach. *Front Cardiovasc Med*. (2019) 6.

5. Mentel A, Quinn TJ, Cameron AC, Lees KR, Abdul-Rahim AZ. The impact of atrial fibrillation type on the risks of thromboembolic recurrence, mortality, major haemorrhage in patients with previous stroke: A systematic review and meta-analysis of observational studies. *Eur Stroke J*. (2020) 5(2):155–68. doi: 10.1177/2396987319896674

6. Clark AL, Coats AJS. Exercise endpoints in patients with chronic heart failure. *Int J Cardiol*. (2000) 73(1):61–6. doi: 10.1016/S0167-5273(99)00223-5

7. Arboiz A, Martí L, Dorison S, Sánchez MJ. Bayés syndrome and acute cardioembolic ischemic stroke. *World J Clin Cases*. (2017) 5(3):93–101. doi: 10.12998/wjcc.v5.i3.93

8. Ali A, Bailey C, Abdelhafiz AH. Stroke prevention with oral anticoagulation in older people with atrial fibrillation—a pragmatic approach. *Aging Dis*. (2012) 3 (4):339–51. Available at: https://pubmed.ncbi.nlm.nih.gov/23185715/

9. Howard PA. Guidelines for stroke prevention in patients with atrial fibrillation. *Drugs*. (1999) 58(6):997–1009. doi: 10.2165/00003495-199958060-00004

10. Björck S, Palaszewsk B, Friberg L, Bergfeldt L. Atrial fibrillation, stroke risk, and warfarin therapy revisited: a population-based study. *Stroke*. (2013) 44(11):3103–8. doi: 10.1161/STROKEAHA.113.002329

11. Ruff CT, Giugliano RP, Braunwald E, Hoffman EB, Deenadayalu N, Ezekowitz MD, et al. Comparison of the efficacy and safety of new oral anticoagulants with warfarin in patients with atrial fibrillation: a meta-analysis of randomised trials. *Lancet*. (2014) 383(9921):955–62. doi: 10.1016/S0140-6736(13)62343-0

12. Vílchez JA, Gallego P, Lip GY. Safety of new oral anticoagulant drugs: a perspective. *Ther Adv Drug Saf*. (2014) 5(1):8–20. doi: 10.1177/2042098613507945

13. Rosenthal L. Atrial fibrillation. *theheart.org* (2019).

14. Seiffge DJ, De Marchis GM, Koga M, Paciaroni M, Wilson D, Cappellari M, *et al*. Ischemic stroke despite oral anticoagulant therapy in patients with atrial fibrillation. *Ann Neurol*. (2020) 87(5):677–87. doi: 10.1002/ana.25700

15. Okumura K, Yamashita T, Akao M, Atarashi H, Ikeda T, Koretsune Y, et al. Oral anticoagulants in very elderly nonvalvular atrial fibrillation patients with high bleeding risks: ANAFIE registry. *JACC: Asia*. (2022) 2(6):720–33. doi: 10.1016/j.jacasi.2022.07.008

16. Gorczyca I, Jelonek O, Michalska-Foryszewska A, Chrapek M, Walek P, Wozakowska-Kapłon B. Stroke prevention and guideline adherent antithrombotic treatment in elderly patients with atrial fibrillation: a real-world experience. *Medicine*. (2020) 99:e21209. doi: 10.1097/MD.0000000000021209

17. Simsek C, Schölzel B, den Heijer P, Vos J, Meuwissen M, Branden B, et al. The rationale of using cerebral embolic protection devices during transcatheter aortic valve implantation. *Neth Heart J*. (2020) 28:249–52. doi: 10.1007/s12471-020-01380-7

18. Haussig S, Linke A, Mangner N. Cerebral protection devices during transcatheter interventions: Indications, benefits, and limitations. *Curr Cardiol Rep*. (2020) 22:96. doi: 10.1007/s11886-020-01335-9

19. Huded CP, Tuzcu EM, Krishnaswamy A, Mick SL, Kleiman NS, Svensson LG, et al. Association between transcatheter aortic valve replacement and early postprocedural stroke. *JAMA*. (2019) 321(23):2306–15. doi: 10.1001/jama.2019.7525

20. Gerckens U, Corrado T, Bleiziffer S, Bosmans J, Wenaweser P, Brecker S, et al. Final 5-year clinical and echocardiographic results for treatment of severe aortic stenosis with a self-expanding bioprosthesis from the advance study. *Eur Heart J*. (2017) 38:278–88. doi: 10.1093/eurheartj/ehx295

21. Gomes WJ, Almeida RMS, Petrucci O, Antunes MJ, Albuquerque LC. The 2020 American College of Cardiology/American Heart Association (ACC/AHA) guideline for the management of patients with valvular heart disease. Should the world jump in? *Braz J Cardiovasc Surg*. (2020) 36(2):502–12. doi: 10.21470/1678-9741-2021-0953

22. Azeem F, Durrani R, Zerna C, Smith EE. Silent brain infarctions, cognition decline: systematic review, meta-analysis. *J Neurol*. (2020) 267(2):502–12. doi: 10.1007/s00415-019-09534-3

23. Davlouros P, Mplani V, Koniari I, Tsigkas G, Hahalis G. Transcatheter aortic valve replacement and stroke: a comprehensive review. *J Geriatr Cardiol*. (2018) 15:95–104. doi: 10.11909/j.issn.1671-5411.2018.01.008

24. Nishimura RA, Otto CM, Bonow RO, Carabello BA, Erwin JP, Fleishera LA, et al. Guideline for the management of patients with valvular heart disease: a report of the American College of Cardiology/American Heart Association task force on clinical practice guidelines. *Circulation*. (2017) 135(25):e1159–95. doi: 10.1161/CIR.0000000000000503

25. Popma JJ, Deeb GM, Yakubov SJ, Mumtaz M, Gada H, O'Hair D, et al. Transcatheter aortic-valve replacement with a self-expanding valve in low-risk patients. *N Engl J Med*. (2019) 380(18):1706–15. doi: 10.1056/NEJMoa1816885

26. Zahid S, Ullah W, Zia Khan M, Faisal Uddin M, Rai D, Abbas S, et al. Cerebral embolic protection during transcatheter aortic valve implantation: updated systematic review and meta-analysis. *Curr Probl Cardiol*. (2022) 101127. doi: 10.1016/j.cpcardiol.2022.101127

27. Deveci OS, Okutucu S, Fatihoglu SG, Oto A. Cerebral embolic protection devices during transcatheter aortic valve implantation, the current state of the art. *Acta Cardiol*. (2022) 77(3):196–203. doi: 10.1080/00015385.2021.1909276

28. Woldendorp K, Indja B, Bannon P, Fanning J, Plunkett B, Grieve S. Silent brain infarcts and early cognitive outcomes after transcatheter aortic valve implantation: a systematic review and meta-analysis. *Eur Heart J*. (2021) 42:1004–15. doi: 10.1093/eurheartj/ehab002

29. Kolte D, Khera S, Nazir S, Butala NM, Bhatt DL, Elmariah S. Trends in cerebral embolic protection device use and association with stroke following transcatheter aortic valve implantation. *Am J Cardiol*. (2021) 152:106–12. doi: 10.1016/j.amjcard.2021.04.038

30. Kawakami R, Gada H, Rinaldi MJ, Nazif T, Leon MB, Kapadia S, et al. Characterization of cerebral embolic capture using the SENTINEL device during transcatheter aortic valve implantation in low to intermediate-risk patients: the SENTINEL-LIR study. *Circ Cardiovasc Interv*. (2022) 15(4):e011358. doi: 10.1161/CIRCINTERVENTIONS.121.011358

31. Isogai T, Vanguru HR, Krishnaswamy A, Agrawal A, Spilias N, Shekhar S, et al. Cerebral embolic protection and severity of stroke following transcatheter aortic valve replacement. *Catheter Cardiovasc Interv*. (2022) 100(5):810–20. doi: 10.1002/ccd.30340

32. Prisco A, Aguado-Sierra J, Butakoff C, Vázquez M, Houzeaux G, Eguzkitza B, et al. Concomitant respiratory failure can impair myocardial oxygenation in patients with acute cardiogenic shock supported by VA-ECMO. *J Cardiovasc Transl Res*. (2022) 15:217–26. doi: 10.1007/s12265-021-10110-2

33. Kassab GS, Choi HW, Navia JA, Jordana J. Devices, systems, and methods for the prevention of stroke, U.S. Patent US9517148B2 (2016).

34. Meyer JS, Charney JZ, Rivera NT, Mathew VM. Cerebral embolization: prospective clinical analysis of 42 cases. *Stroke*. (1971) 2(6):541–54. doi: 10.1161/01.STR.2.6.541

35. Hernandez SAR, Kroon AA, van Boxtel MPJ, Mess WH, Lodder J, Jolles J, et al. Is there a side predilection for cerebrovascular disease? *Hypertension*. (2003) 42 (1):56–60. doi: 10.1161/01.HYP.0000077983.66161.6F

36. Riegel J, Mayer W, Havre YV. Freecad (2022).

37. Choi HW, Navia JA, Kassab GS. Thrombus deflector stent for stroke prevention: a simulation study. *J Biomech*. (2015) 48(10):1789–95. doi: 10.1016/j.jbiomech.2015.05.006

38. Paschoalino WJ, Payne NA, Pessanha TM, Gateman SM, Kubota LT, Mauzeroll J. Charge storage in graphene oxide: impact of the cation on ion permeability and interfacial capacitance. *Anal Chem*. (2020) 92(15):10300–7. doi: 10.1021/acs.analchem.0c00218

39. Alpert JS, Petersen P, Godtfredsen J. Atrial fibrillation: natural history, complications, and management. *Annu Rev Med*. (1988) 39:41–52. doi: 10.1146/annurev.me.39.020188.000353

40. Bagur R, Solo K, Alghofaili S, Ombela-Franco L, Kwok CS, Hayman S, et al. Cerebral embolic protection devices during transcatheter aortic valve implantation: systematic review and meta-analysis. *Stroke*. (2017) 48:1306–15. doi: 10.1161/STROKEAHA.116.015915